– 8 –

Physical Principles of Resonance Methods in Chemistry

8.1 SELECTED ATOMIC NUCLEI CHARACTERISTICS

So far we have considered the atomic shell and the point (dimensionless) nucleus with charge *Ze* interacting with electrons by Coulomb forces according to the laws of quantum mechanics. The account of the nuclei characteristics with a definite dimension raises many important and interesting phenomena. They are the basis of modern methods of investigation of atomic and molecular structure of chemical substances.

The aim of the present chapter is to give relevant information on the atomic nucleus. Taking into account the general aim of the book, we will only touch on those nuclei properties, which have a direct bearing on the description of methods, so this information cannot be considered as comprehensive.

Among the modern chemical and physical methods of investigation, spectroscopic methods are widely used (they are often called instrumental methods). These methods allow quantitative information on composition and structure to be obtained effectively and rapidly, and also enable analytical and other problems to be solved without the destruction of the materials tested. Further, these methods are in the process of development and improvement.

Very popular among these methods are the nuclear resonance (spectroscopic) methods, which are based on the fundamental discoveries made in quantum mechanics and radioengineering in the second part of the 20th century, namely, nuclear magnetic resonance (NMR), nuclear quadrupole resonance (NQR), γ-resonance (Mössbauer) spectroscopy (ΓRS), electron paramagnetic resonance (EPR), and others.

As these resonance methods are based on electron–nuclear interactions, we must provide some information on the nuclear physics required to understand the subject.

8.1.1 A nucleon model of nuclei

A nucleus possesses an internal structure. It consists of many elementary particles—nucleons—the main of which are protons and neutrons. They move in the field of nuclear forces and continuously change their state from that of charged particle (proton) to neutral particle (neutron) and back. However, on an average in a given nucleus, a certain number

of protons, Z (which defines the given element's number in the periodic system) and number of neutrons, N (which defines the particular isotope of a given element) are always present. Since the mass of protons and neutrons are approximately 2000 times greater than the mass of electrons, the total mass of an atom is practically comprised in its nucleus. The total number of nucleons, A, is called the mass number, i.e., $A=N+Z$.

The symbol ${}^{A}Z_{N}$ is used to identify a nucleus, where Z is the chemical symbol of a given element. Mass number A defines the mass of a nucleus. Thus, there are 92 protons and 143 neutrons in the uranium nucleus ${}^{235}U_{92}$. The number of nucleons Z is often omitted because the relevant information is contained in its chemical symbol. Thus, ${}^{235}U$ is the usual symbol. In the text below, a proton mass is marked by m_p. Mass can be measured in kilograms ($m_p=1673\times10^{-27}$ kg), or can be denominated in atomic units of mass (1 a.m.u.$= 1.66\times10^{-27}$ kg). It is sometimes also expressed in energy units ($m_p=938.2$ MeV).

Each nucleon possesses its own angular momentum, i.e., spin**.** The quantum numbers of neutron and proton spins are the same as an electron spin, i.e., 1/2. In general, a complex nucleus also possesses a spin angular momentum. As a result of the partial or complete compensation of nucleonic spins, the total spin can have values of 0, 1/2, 1, 3/2, etc. Herewith, in full analogy with the electronic shell, the angular moment (mechanical moment) of a nucleus is:

$$L_I = \hbar\sqrt{I(I+1)}, \tag{8.1.1}$$

where I is the spin quantum number of a particular nucleus.

Analogously with electron characteristics, the projection L_I on the selected axis z can have the values:

$$L_z = \hbar m_I, \tag{8.1.2}$$

where quantum number $m_I = I, I-1, \ldots 0, \ldots -I$ can have $2I + 1$ values. From eqs. (8.1.1) and (8.1.2), it can be seen that the value of electron and nucleon angular momentums have the same order ($\sim\hbar$).

Because the nucleus spin is stipulated by the behavior of both neutrons and protons, the existence of nuclear magnetic momentums can be expected as well. The vectors of mechanical and magnetic moments are tightly bonded to each other. Nuclear physics was developed much later than atomic physics and this fact has influenced the approach to the description of nuclear properties. So, eq. (5.2.2), describing the electron gyromagnetic ratio of magnetic to mechanical moments, is applied to the nuclei as well. As a result, the gyromagnetic ratio for a spin-possessing nuclei was formally transcribed as:

$$\frac{\mathcal{M}}{L_I} = g_N \frac{|e|}{2m_p} \tag{8.1.3}$$

(in SI), however, instead of the mass of electron m_e in the denominator, the proton's mass m_p is present. Hence, the magnetic moment of a nucleus can be derived as:

$$\mathcal{M}_I = g_N \frac{|e|\hbar}{2m_p}\sqrt{I(I+1)} \tag{8.1.4}$$

The value

$$\frac{e\hbar}{2m_p} = \mu_N \tag{8.1.5}$$

is referred to as the nuclear magneton and denoted as μ_N ($\mu_N = 5.05 \times 10^{-27}$ J/T).

Since in nuclear physics the mutual orientation of the angular and magnetic moments can be both parallel or antiparallel, the gyromagnetic ratio can also be positive (parallel orientation of these two vectors) and negative (antiparallel orientation as for orbital electron state). Therefore, the nuclear g-factor (g_N) (in units $e/2m_p$) can have both positive and negative signs. They cannot be calculated but are defined from experiment only. Therefore, one can see that the g_N sign is historically casual. For proton g_p is $+5.5851$, for neutron $g_N = -1.9103$.

It can be seen from eqs. (8.1.4) and (8.1.5) that the magnitudes of the nuclear magnetic moment are approximately 2000 times lower than the corresponding electron values. Therefore, special instruments are necessary for observing them.

The z-projection of $\mathcal{M}_I$ is:

$$\mathcal{M}_{Iz} = g_N \mu_N m_I \tag{8.1.6}$$

Because $\mathcal{M}_I$ and L_I are tightly bonded, nuclei precession in the magnetic field also takes place (refer to Section 5.2.4). The magnetic field created by electron shell can in this case be regarded as external to the nucleus.

It is necessary to note that the nature of the nucleon's magnetism is still not sufficiently clear. For instance, it is not understood why such an electrically neutral particle as a neutron nevertheless possesses a magnetic moment.

8.1.2 Nuclear energy levels

One of the distinctive signs of any quantum mechanical system, including nuclei, is the discontinuity of its energy states. The permitted values of nuclear energy depend on its particular structure, the nature of the nuclear forces, and more. Unfortunately, at present, nuclear physics does not allow us to calculate theoretically the arrangement of energy levels; these are experimentally found values.

Nuclear ground states E_0 are stable, not changing their energy in the course of time. However, by one or other external influence, they can be excited to states E_1, E_2, etc. All

excited states are unstable: in the course of time, nuclei spontaneously transform to the lower or ground state, emitting in the surrounding space an excess of energy in the form of γ rays. The time during which the number of originally existing nuclei decreases in e times is referred to as the nuclear lifetime τ. For a given nucleus in different excited states, τ can have widely different values, however, a quantum mechanical relationship always exists between the value τ and uncertainty of energy ΔE in the given energy state (refer to Section 7.2).

$$\tau \Delta E \geq h. \tag{8.1.7}$$

For instance, if $\tau=\infty$ (ground state), energy E_0 can have a precise value ($\Delta E=0$). If $\tau\sim10^{-8}$ sec, then $\Delta E\sim10^{-7}$ eV. Usually, relative to E_0, the first excited energy levels of many nuclei are $E_1-E_0\sim10^4$ eV. Therefore, the ratio $\Delta E/(E_1-E_0)$ is of 10^{-11} in the order of value and seemingly can be regarded as negligible. However, as we will see below, this is not so.

8.1.3 Nuclear charge and mass distribution

The distribution of neutrons and protons in a nucleus can be different. In the majority of experiments, a nucleus behaves as a system possessing a center of symmetry and axis of symmetry of an endless order. Consequently, a nucleus also possesses a mirror plane of symmetry perpendicular to the symmetry axis passing through the center of symmetry.

The charge distribution can be described by the function of the charge density $\rho(x,y,z)$. The normalization of the charge to the total nuclear charge gives:

$$\int_V \rho(r)dv = Ze, \tag{8.1.8}$$

The distinctive features can be mentioned in this description. Firstly, the average density function can differ for charge and mass distribution. If, in particular, protons are distributed at the nucleus periphery and neutrons are concentrated nearer the origin, the characteristic radii of the two can be different. They can differ even for the two energy states of one and the same nucleus. Secondly, the nuclear forces are of short-range nature. Therefore, nuclei are sharply outlined in space. There is an empirical expression for spheri cal nuclei size:

$$r_{\text{я}} \approx 1.25\times10^{-15}\sqrt[3]{A}\ \text{m}, \tag{8.1.9}$$

where A is the mass number. Thirdly, the nucleus can deviate from the spherical symmetry toward the ellipsoid of revolution with three mutually perpendicular second-order symmetry axes. Such an ellipsoid is of two radii: a is directed along z-axis and b is perpendicular to it. The ellipsoids of revolution can be flattened ($a<b$) or elongated ($a>b$) (Figure 8.1).

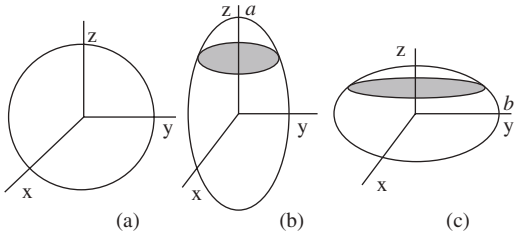

Figure 8.1 Models of different nuclear forms: (a) spherical, (b) elongated and (c) flattened.

8.1.4 Nuclear quadrupole electrical moment

Point charge and dipole electrostatic fields have been described in Chapter 4. There are more complex electrical systems created by irregularly distributed charges (refer to Appendix 3). It is shown in Appendix 3 that such a system can produce an electrostatic field, which can be described by the sum of terms differently dependent on the distance r (Table 8.1).

Being charged, the nucleus has nonzero monopole contribution. Since nuclei possess the definite symmetry elements listed above, it cannot possess a dipole moment; a dipole moment as a vector cannot coexist with the symmetry operations mentioned. This signifies that the nucleus does not possess a dipole moment.

However, this does not prohibit a nucleus from having an electrical multipole moment of higher order: quadrupole, in particular. In other words, the deflection of the nucleus from a spherical form brings about the existence of the quadrupole moment eQ (refer to Appendix 3). Value eQ is measured in $C{\cdot}m^2$ units (in SI).

The mathematical description of the quadrupole moment can be given as:

$$\iiint_V \rho(x,y,z)(3z^2 - r^2)dV = eQ \tag{8.1.10}$$

where $r^2 = x^2 + y^2 + z^2$, $dV = dx\,dy\,dz$. Integration is subjected over the whole nucleus volume V. Bearing in mind that in the reference system connected with the nucleus (refer to Figure 7.16), this expression can be presented in trigonometric form:

$$eQ = \iiint_V \rho(x,y,z)r^2(3\cos^2\theta - 1)dV. \tag{8.1.11}$$

As shown in Appendix 3, the charged system elongated up to the z axes possesses a positive quadrupole moment, though for the flattened nucleus it is negative.

The deflection of the nucleus from a spherical form and the nucleus spin are interrelated. Therefore, one can expect that the experimental manifestation of a quadrupole moment and nuclear spin are also correlated. This is exhibited in the following. The uncertainty in the angular momentum orientation (see Figure 7.17) is present in the quadrupole moment

Table 8.1

Properties of a number of electric systems

Charges system	Electric field E as dependent on distance r	Potential φ as dependent on distance r	Energy in an external electric field
Monopole	$E_c \sim \frac{q}{r^2}$	$\varphi_c \sim \frac{q}{r}$	$U \sim q\varphi$
Dipole	$E_d \sim \frac{p}{r^3}$	$\varphi_q \sim \frac{p}{r^2}$	$U \sim p\frac{d\varphi}{dr}$
Quadrupole	$E_q \sim \frac{qa^2}{r^4}$	$\varphi_q \sim \frac{qa^2}{r^3}$	$U \sim qa^2\frac{d^2\varphi}{dr^2}$

too. The measured value is not the eQ itself but the quantity eQ_z that can be expressed through the nuclear spin I as:

$$eQ_z = \frac{I-(1/2)}{I+1}eQ. \tag{8.1.12}$$

This means that at $I=0$, the quadrupole term is meaningless; at $I=1/2$, it cannot be measured and it is reliably measured at $I>1/2$.

8.2 INTRAATOMIC ELECTRON–NUCLEAR INTERACTIONS

8.2.1 General considerations

If we consider a nucleus being not a point but a volumetric nucleus, additional effects in the electron–nucleus interaction appear. They play a very important role in the physical description of an atom. These additional effects are exceedingly small in comparison with the main Coulomb and even with fine interactions (refer to Section 7.5.4). So, they refer to the number of intraatomic "superfine interactions."

Remember that the energy of the electrostatic interaction of two electric charges is defined by product $q\varphi$ (refer to Section 4.1.4) in which φ is a potential created by the electron's charge in the point where the proton's charge is located. Therefore, the additional interaction energy appears. (Certainly one can consider that the field is created by a volumetric nucleus and an electron is in this field; this effect will also be considered further.) The most general expression for the electrostatic (marked by letter E) interaction energy can be written as:

$$E_E = \iiint_V \rho(x_1,x_2,x_3)\varphi(x_1,x_2,x_3)dx_1\,dx_2\,dx_3. \tag{8.2.1}$$

For convenience in this expression, instead of Cartesian coordinates x,y,z we can choose another form of coordinates $x_1 \to x$, $x_2 \to y$, $x_3 \to z$. The function that describes a charge distribution in a nucleus is $\rho(x_1,x_2,x_3)$, the potential created by the electron shell at the nucleus is denoted $\varphi(x_1,x_2,x_3)$, and the integral is taken upon the whole nucleus volume V.

Decomposing the function $\varphi(x_1,x_2,x_3)$ in the MacLoren series near the origin:

$$\varphi(x_1,x_2,x_3) = \varphi(0,0,0) + \sum_{\alpha=1}^{3}\left(\frac{\partial\varphi}{\partial x_\alpha}\right)_0 x_\alpha + \frac{1}{2}\sum_{\alpha=1}^{3}\left(\frac{\partial^2\varphi}{\partial x^2}\right)_0 x_\alpha^2 + \frac{1}{2}\sum_{\alpha=1}^{3}\sum_{\beta=1}^{3}\left(\frac{\partial^2\varphi}{\partial x_\alpha \partial x_\beta}\right)_0 x_\alpha x_\beta \cdots \tag{8.2.2}$$

where $(\partial\varphi/\partial x_\alpha)_0$ are electric field components along the axis x_α, $(\partial^2\varphi/\partial x_\alpha^2)_0$ are the electric potential gradient along the same axis. Because of the small dimension of nuclei, it is possible to limit the number of terms in expression (8.2.2) by the second order.

The electric field gradient possesses the symmetry axis along the x_3 axis. Therefore, all crossed terms of the type $(\partial^2\varphi)/(\partial x_\alpha \partial x_\beta)$ with $\alpha \neq \beta$ are equal to zero.

Substituting the expression (8.2.2) into the electric energy (8.2.1) we have:

$$E_E = \iiint_V \rho(x_1,x_2,x_3)\left\{\varphi(0,0,0) + \sum_{\alpha=1}^{3}\left(\frac{\partial\varphi}{\partial x_\alpha}\right)_0 x_\alpha + \frac{1}{2}\sum_{\alpha=1}^{3}\left(\frac{\partial^2\varphi}{\partial x_\alpha^2}\right)_0 x_\alpha^2\right\} dx_1\, dx_2\, dx_3 \tag{8.2.3}$$

Opening the brackets and carrying out elementary transformation we obtain:

$$E_E = \int \rho(x_1,x_2,x_3)\varphi(0,0,0)dV + \sum_{\alpha=1}^{3}\left(\frac{\partial\varphi}{\partial x_\alpha}\right)_0 \cdot \int \rho(x_1,x_2,x_3)x_\alpha dV + \frac{1}{2}\sum_{\alpha=1}^{3}\left(\frac{\partial^2\varphi}{\partial x_\alpha^2}\right)_0 \cdot \int \rho(x_1,x_2,x_3)x_\alpha^2 dV + \ldots \tag{8.2.4}$$

For our convenience, let us write every term separately presenting eq. (8.2.4) as a sum $E_E = E_{E_1} + E_{E_2} + E_{E_3}$ and then:

$$E_{E_1} = \int \rho(x_1,x_2,x_3)\varphi(0,0,0)dV$$

Because $\varphi(0,0,0)$ is the electric potential at the origin, it is the number and can be taken out from the integral. The rest is the nucleus charge, Ze. Therefore,

$$E_{E_1} = eZ\varphi(0,0,0), \tag{8.2.5}$$

The first term in eq. (8.2.5) E_{E_1} is the interaction energy of atomic electrons with the nucleus, the charge of which is contracted to point; the nucleus becomes dimensionless.

Integrals of the type $E_{E_2}=\int\rho(x_1,x_2,x_3)x_\alpha dV$ in (8.2.4) are equal to zero because of the fact that according to their mathematical structure, they describe nuclear electric dipole moments though we already know that the nucleus cannnot have one. Therefore, eq. (8.2.4) reduces to two terms, the first and the third:

$$E_E = eZ\varphi(0,0,0)+\frac{1}{2}\sum_{\alpha=1}^{3}\left(\frac{\partial^2\phi}{\partial x_\alpha^2}\right)_0\int\rho(x_1,x_2,x_3)x_\alpha^2 dV, \tag{8.2.6}$$

By some transformations, the term E_{E_3} can be transformed into the sum:

$$E'_{E_2} = \tfrac{2}{3}\pi e^2 Z\,|\psi(0)|^2\,\langle r^2\rangle \tag{8.2.7}$$

and

$$E''_{E_3} = \frac{1}{4}\varphi_{zz}[eQ]\frac{3m^2-I(I+1)}{3I^2-I(I+1)}. \tag{8.2.8}$$

Consider all terms separately. We will refer here to the energy level scheme in Figure 8.2.

8.2.2 Coulomb interaction of an electron shell with dimensionless nucleus

The first term in (8.2.4) (E_{E_1} in eq. (8.2.5)) describes the electrostatic interaction of an electron shell with the point nucleus charge at the origin (Figure 8.2a). This term corresponds fully to the Coulomb energy, which was discussed in Section 7.5; hence, the quantization of the energy is just the same as was accepted above. In other words, E_1 is the energy that describes the electron shell state in the absence of superfine interactions.

Evaluation of the energy has already been made in Section 7.5.4. It shows that depending on Z, the energy E_{E_1} is 10^1-10^4 eV. Remember that the addition to E_{E_1}, the energy of spin–orbit fine interactions is $\Delta E_{nj}\sim 10^{-1}/10^{-3}$ eV.

Other types of interactions have made their own particular contribution to the energy levels.

8.2.3 Coulomb interaction of an electron shell with a nucleus of finite size: the chemical shift

Let us consider the next term eq. (8.2.7). Two multipliers exist in this term: $\langle r^2\rangle$ is the mean-square nuclear charge radius (determined according to the general rule (eq. (3.1.6′)) $\langle r^2\rangle=(\int\rho(x_1,x_2,x_3)r^2dv)/(\int\rho(x_1,x_2,x_3)dv)$ and $|\psi(0)|^2$ is the probability density of finding an electron at the origin. Notice that this term accounts for the nonzero nuclear size.

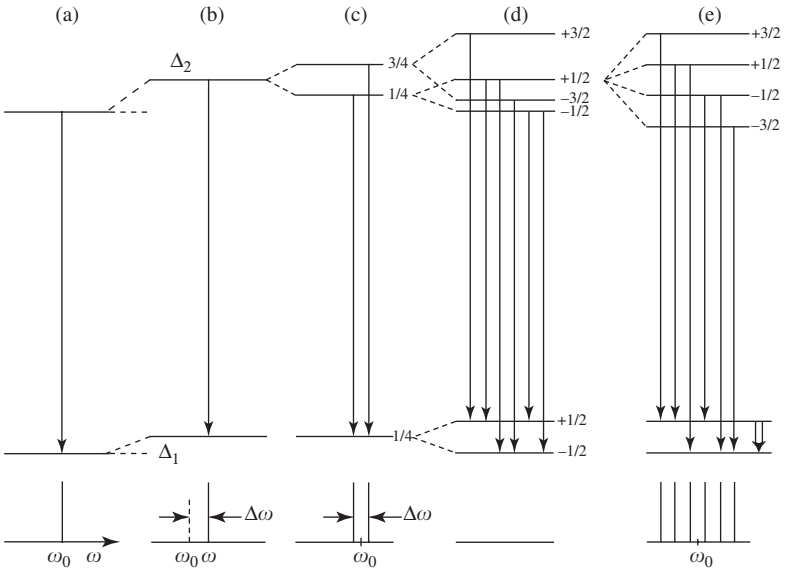

Figure 8.2 The particular effects influences on the energy state of an atom: (a) a stripped nucleus, (b) the chemical shift (refer to Section 8.2.3), (c) the fine electron-nucleus interaction (refer to Section 7.5.8), (d) and (e) an atom in an external magnetic field (in (d) influence of both quadrupole and magnetic splitting is very complicate), (e) the influence of the magnetic field produced by the electron shell on the nucleus's magnetic moment position (nuclear Zeeman effect, see Section 7.7). The shift of the spectral line relative ω_0 is presented in the lower part of the Figure. The energy transitions scale is not followed. The long arrows represent ΓR transitions, the double arrow in the figure represent the NMR transitions.

It follows from eq. (8.2.7) that this energy contribution characterizes the electron cloud interaction with the nuclear charge. This type influences the shifting of the nuclear energy levels but does not split them. The energy shift depends on a product: the electronic parameters $[e|\psi(0)|^2]$ and the nuclear properties $(Ze\langle r^2\rangle)$ (Figure 8.2b). Because nucleus excitation can lead to a change of its mean-square radius $\langle r^2\rangle$, this value can differ for two levels—the ground and the excited ones. Therefore, the energy difference can be changed. This phenomenon is referred to as the *chemical shift.* The experimental spectral lines are schematically shown under the energy transitions.

Analysis of the electron radial curves (Figure 7.22 and Table 7.1) shows that only s-electrons can influence the $|\psi(0)|^2$ value. In the isolated atom, the energy E'_{E_2} could change the line position only a little. This is schematically shown in Figure 8.2b. The E'_{E_2} value is often 10^{-4} eV and has a positive sign. The difference between the energy of two levels is significantly smaller than the energy itself and is usually 10^{-7}–10^{-8} eV. As a result, the line position on the experimental spectrum is shifted as well by $\Delta\omega$, as shown in the figure.

For a given atom in different atomic groups and/or molecules, the E'_{E_2} value can be changed. When an atom enters the chemical bonding with other atoms, it produces new molecules and the whole electron system undergoes a change (s-electrons including). This last influences the E'_{E_2} value. Thus, the chemical shift is a very sensitive measure of the chemical bonding.

It is impossible at present to calculate the E'_{E_2} value theoretically. However, the change in the energy transition can be found experimentally. In order to give this value a quantitative character, measurements are carried out relative to a specially chosen reference substance. In this case, one can measure the quality:

$$E'_{E_2} = Ze^2\pi\langle\Delta r^2\rangle\{|\psi(0,0,0)|^2 - |\psi(0,0,0)|^2_{\text{refr}}\}, \tag{8.2.9}$$

where $\langle\Delta r^2\rangle = \{\langle r^2_{\text{excited}}\rangle - \langle r^2_{\text{ground}}\rangle\}$ is the change of the mean-square nuclear charge radius in the transition from the excited to the ground state. As soon as the reference substance is chosen (the second term in the difference in the figure bracket), the E'_{E_2} quality is called the chemical shift relative to a definite compound.

In modern chemistry, the chemical shift is one of the main, widely used characteristics of an atom in a molecule.

Measurement of the chemical shift can be achieved by means of NMR and ΓR. It should be noticed, however, that the specificity and individual development of these two methods are the reason that different data and different reference substances determine the difference in results, although the physical content of both methods remains the same.

8.2.4 The nuclear quadrupole moment and the electric field gradient interaction

A second term in eq. (8.2.6) corresponds to the so-called quadrupole effects related to electron–nuclear superfine interactions. Unlike the preceding, it brings about the splitting of nuclear energy levels into sublevels, lying both above and below the main level because the energy of this interaction can have both positive and negative signs. As well as chemical shift, the quadrupole interaction expression consists of two terms: one describes the nucleus feature, i.e., the nuclear quadrupole moment, and the others present the electrical field gradient in the point where the nucleus is located $(\partial^2\varphi/\partial x^2_\alpha)_0 = (\partial E/\partial z)_0$ The nuclear quadrupole moment was considered in the previous chapter (refer to formulas (8.1.10) and (8.1.11)). It depends on the quantum numbers I and m_I: depending on these numbers, the originally singular level splits into several sublevels (degeneration on the quantum number m_I is partly lifted). The scheme of quadrupole splitting with the nuclear spin $I=3/2$ is given in Figure 8.2c. Since in the expression for the energy, the square of quantum number m_I is entered, the four values of m_I ($\pm 1/2$ and $\pm 3/2$) correspond only to two energy levels. When a system turns from the upper (split) onto the ground (singular) level, two lines appear (as shown in Figure 8.2c). The distance between sublevels depends on the electrical field gradient at the nucleus. These are called *quadrupole* splitting.

In order for quadrupole splitting to be developed two conditions must be fulfilled. First, the nucleus must possess a quadrupole electric moment (refer to eq. 8.1.10). Second, it is necessary for the nucleus be in the point where the electric field gradient exists. This appears in those cases where an atom is in an asymmetric environment. Thus, a relationship of the quadrupole splitting and the chemical structure appears.

Unlike the chemical shift, which depends only on s-electrons, the gradient of an electrical field can be created by p-, d- and f -and other electrons.

The evaluation of the value developed in this splitting is usually in the order of $10^{-7}-10^{-8}$ eV.

It is possible to observe nuclear quadrupole splitting using ΓR and NQR methods.

8.2.5 Interaction of a nuclear magnetic moment with an electron shell

In addition to the electrostatic interactions of a nuclear charge with an atomic electron shell, there is also the interaction of a nuclear magnetic moment with a magnetic field created by an electronic shell at the point of nucleus location. Two phenomena appear simultaneously: the electron shell creates a magnetic field at the point of nucleus location, and, on the other hand, the nuclear magnetic moment creates a magnetic field influencing the electron cloud.

The interaction of the nuclear magnetic moment with the electron magnetic field can be described by the Zeeman effect (refer to Section 7.7). The Zeeman splitting in this instance is:

$$E_{\mathrm{M}} = g_{\mathrm{N}} m_I \mu_{\mathrm{N}} B(0,0,0), \tag{8.2.10}$$

where $B(0,0,0)$ is the magnetic field induction produced by electrons at the origin.

In magnetically disordered materials, as a result of the thermal chaotic motion of atoms, the averaged nuclear magnetic field is zero and the effect is nonobservable. In magnetically ordered materials, the chaotic motion does not occur in full measure and a nuclear Zeeman effect takes place.

In this case, the degeneration upon m_I is lifted (refer to Section 7.7), i.e., the nuclear energy level with a certain I is split into $2I+1$ sublevels. Figure 8.2e presents such spectral lines splitting with $I=3/2$: this level will form six equidistant superfine magnetic splitting lines. The splitting energy $\Delta\omega''$ is defined by an expression close to eq. (7.7.5).

It can be seen from expression (8.2.10) that the additional energy of the magnetic interaction depends on the magnetic field imposed on the nucleus. Because the nucleus magnetism is 1840 times lower than the electronic, the Zeeman nuclear splitting is significantly less than the electronic. However, owing to the large magnitude of the magnetic field created by electron shell at the nucleus position, this splitting can be experimentally observed, for instance, by the γ-resonance method.

The same happens when the nuclear magnetic moment acts on the atomic electron's shell. This makes it possible to investigate the changes in the shell caused by the chemical interactions.

8.2.6 Atomic level energy and the scale of electromagnetic waves

Let us analyze the results. A general scheme of nuclear energy levels with consideration of all electronic–nucleus interactions is given in Figure 8.2. A scheme corresponding to idealized models of stripped nucleus (without electronic shell) is given in Figure 8.2a. As an example, the energy states—ground and excited—were accepted with quantum numbers $I = 1/2$ and 3/2, accordingly. The excitation energy for the majority of cases is of the order 10^4 eV.

When a nucleus undergoes transformation from an excited to a ground state, a γ-quantum is emitted, the frequency of which is $\omega=(E_{3/2}-E_{1/2})/\hbar$. For stripped nucleus, we denote this frequency as ω_0.

If we put the originally taken nucleus of nonzero size into the usual electronic shell and observe the interactions, we should take the Coulomb forces of the nucleus with electrons into account (eq. (8.2.5)) (Figure 8.2b). This event shifts both levels. The displacement value is in the order of 10^{-4} eV. (Attention should be paid to the fact that it is impossible to draw the levels and splitting in Figure 8.2 to the right scale: on the background of main transition 10^4 eV, we must depict details of $10^{-7}-10^{-8}$ eV, the difference is 11 orders of value less.) However, it is important that the nucleus in ground and excited states can have different radii (different root mean square radii $\langle r^2\rangle$) and displacements of those two levels are different (however, $|\varphi(0,0,0)|^2$) in both cases is the same). Measurements show that this difference is of the order 10^{-7} eV. So, transition frequency ω decreases by the value $\Delta\omega\sim10^{-7}/10^{-15}\sim10^8$ Hz (in comparison with 10^{19} Hz).

The next step is an account of quadrupole interaction (eq. 8.2.8) provided the nucleus possesses a quadrupole moment and is in a nonuniform electric field. If both these conditions are fulfilled, the energy levels split according to eq. (8.2.8) (see Section 8.2.4). When quantum number m_I present in this expression is in square, the top level splits into two sublevels ($m_I^2 = 9/4$ and 1/4) and the lower level does not split at all ($m_I^2 = 1/4$). Therefore, one existing spectral line splits in two. The experimental evaluations show that the usual value of quadrupole splitting is about 10^{-7} eV.

If one takes into consideration the magnetic field created by the electronic shell at the nucleus position (Figure 8.2d), the scheme of energy transitions becomes more complicated (see Section 8.2.5). The degeneration on m_I is lifted. The value of splitting is defined by the particular magnitudes of the terms in eq. (8.2.4). If the magnetic and quadrupole contributions are presented simultaneously, the spectral picture gets more and more complex (not shown in Figure 8.2d).

If we consider magnetic splitting alone, the spectral picture gets comparatively simple (Figure 8.2e). Here, we should keep in mind that the selection rules permit only the transition for which quantum number m_I is changed to unity or is not changed at all. If we take $I=(3/2)$, the spectrum will split into six lines. The magnitude of splitting depends on the nuclear g-factor and on magnetic field induction at the nucleus position.

In addition to the transition between sublevels of excited and ground states, other transitions are also possible, in particular between two sublevels of a single ground state (the double arrow in Figure 8.2e). The single arrows correspond to ΓRS and the double arrows describe the NMR.

8.3 γ-RESONANCE (MÖSSBAUER) SPECTROSCOPY

8.3.1 Principles of resonance absorption

In certain circumstances, a substance is capable of absorbing electromagnetic energy, particularly, powerfully and selectively. This happens when the energy of a falling quantum coincides with the electron and/or nuclear energy level difference. Then, so-called *resonance absorption* of the electromagnetic radiation occurs.

Suppose that the sample contain atoms with two intrinsic energy levels E_1 and E_0. The resonance condition can be written as:

$$E_1 - E_0 = \hbar\,\varpi_{\text{res}} = g_{\text{N}}\mu_{\text{N}}B, \tag{8.3.1}$$

(remember that the change in quantum number Δm_I is ± 1). Here, B is the magnetic induction at the nucleus position.

An experimental scheme is depicted in Figure 8.3. In Figure 8.3a, the main parts of the experimental equipment are shown: an emitter (1), a sample (2) and a detector (3). The resonance is observed when condition (8.3.1) is met. In Figure 8.3b, the absorption curve is

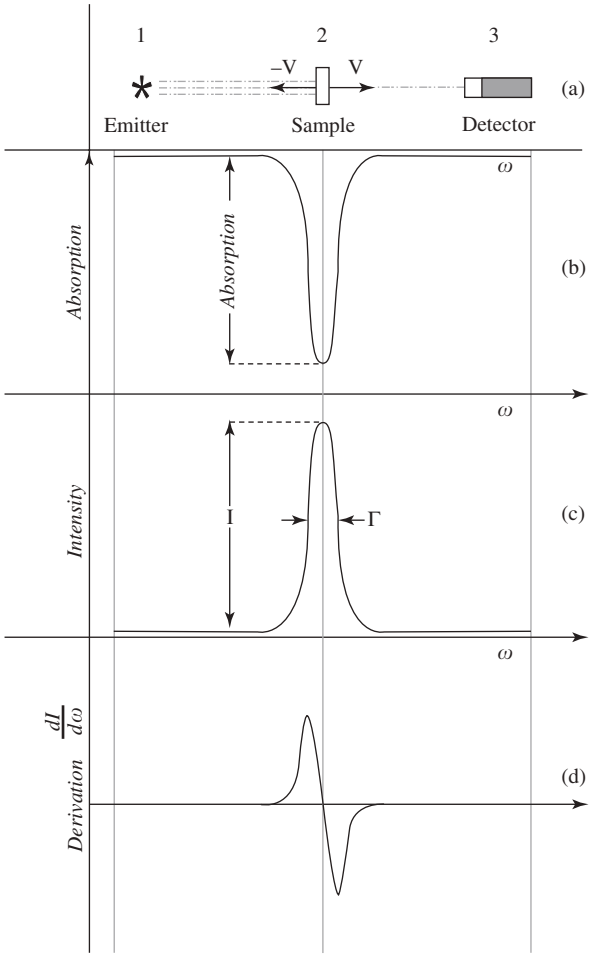

Figure 8.3 An experimental arrangement of the γ-resonance experiment: (a) experimental arrangement, (b) absorption curve, (c) transmission curve and (d) $dI/d\omega$ curve. Γ is the width of a bell-like curve on the half-height (half-width).

presented, whereas in (c) the transmission is depicted. Only a single frequency ω can be found in experiments. In order to measure the whole curve and reveal reliably resonance absorption, a displacement from the resonance frequency should be accomplished. The frequency ω can be changed although it is easier to move the emitter (or sample) relative to each other using the Doppler effect. In some cases, the derivative curve is measured (Figure 8.3d).

The point is that if both emitter and detector are motionless, the device would register γ quanta with just the emitted frequency. If either the emitter or detector begins to move along the connecting straight line with relative velocity V, the harmony is destroyed. Depending on V, the detector will register another frequency ω'. The difference $\omega-\omega'=\Delta\omega$ can be found according to the Doppler effect (refer to Section 2.8.4 and to eq. (2.8.23)), namely,

$$\omega' \approx \omega_0\left(1+\frac{V}{c}\right)=\omega_0+\omega_0\frac{V}{c}, \tag{8.3.2}$$

The resonance curve is characterized by several parameters: position, width on half of the height (half-width) and intensity (height of maximum or absorption "depth").

8.3.2 Resonance absorption of γ-rays: Mössbauer effect

Assume that there are two samples with exactly the same structure and nuclei. This signifies that the positions of two energy levels in both samples are exactly equal. Assume further that there is a way to initiate the nuclei of the first sample to emit γ quanta. The emitted spectral line $E_1-E_0=\Delta E$ will exhibit a frequency, ω. One can evaluate the value of the natural width of this spectral line (i.e., the width as defined by quantum physics (refer to Chapter 7.2) but not by imperfection of the experimental equipment). The uncertainty principle gives:

$$\Gamma=\frac{\hbar}{\tau}=\frac{10^{-15}c}{10^{-7}c}=10^{-8}\,\text{eV} \tag{8.3.3}$$

where Γ is the natural half-width of the spectral line and τ is the average time-of-life of a nucleus in an excited state with the energy E_1. The ratio of the natural half-width to the absolute energy value will then be $\Gamma/(E_1-E_0)\approx(10^{-8}\text{ eV}/10^{-4}\text{ eV})\approx10^{-12}$. It can be seen that this relative width is very narrow.

If this radiation is directed onto a second quite similar sample, resonance should occur, i.e., the resonance absorption should be observed. Indeed, the γ-quantum energy is precisely equal to the energy difference E_1-E_0. The absorption of the electromagnetic waves with γ-quantum energy just equal to the energy difference in a sample is caused by the resonance absorption, i.e.:

$$\omega_{\text{res}}=\frac{E_1-E_0}{\hbar} \tag{8.3.4}$$

If it is possible to change smoothly the electromagnetic radiation frequency, then the resonance radiation absorption can be observed in the background of the nonresonance processes. Such an experimental scheme is depicted in general form in Figure 8.3.

However, there are at least two factors that destroy the resonance. The first factor is recoil, which obtains free nucleus when emitting the γ quantum. Really, the law of momentum conservation requires that the total system momentum, being equal to zero before emitting the γ quantum ($0=p_\gamma+p_n$), should be kept at zero after disintegration, so

$$0 = p_\gamma + p_n \quad \text{or} \quad p_\gamma = -p_n, \tag{8.3.5}$$

where p_γ and p_n are the $p_\gamma-$ and p_n-nuclear momentums. The law of energy conservation in this case has the form $E_2-E_1=E_\gamma+E_n$, where:

$$E_\gamma = (E_2 - E_1) - E_n \tag{8.3.6}$$

It can be seen that the γ-quantum energy E_γ is less than the ideal value E_1-E_0, on the value of nucleus recoil energy E_n (denoted usually as R). From eqs. (8.3.5) and (8.3.6), we can find values $E_n \equiv R$. The energy of a photon is correlated with its momentum by the equation (see Chapter 1.6):

$$E_\gamma = p_\gamma c \tag{8.3.7}$$

where c is the speed of light. Energy of recoil, R, from the above given equations is

$$R = \frac{p_N^2}{2m_N} = \frac{p_\gamma^2}{2m_N} = \frac{E_\gamma^2}{2m_N c^2} \sim 10^{-3} - 10^{-2}\ \text{eV} \tag{8.3.8}$$

This signifies that the emitting line is displaced along the energy axis on R to a side of its reduction. This shift itself is small, particularly in comparison with the quantum energy (10^4 eV); however, in comparison with the natural width of a spectral line (10^{-8} eV), it is large. Similarly, the spectral absorption line will be displaced as well, but in the opposite direction. Two lines, the natural width of which are 10^{-8} eV, move apart by 10^{-3} eV (Figure 8.4). Thereby, no overlap of the spectral lines takes place, and, consequently, no resonance absorption occurs.

The second factor is chaotic thermal atomic motion: different nuclei are emitted in different chaotic states of movement. As a result of the Doppler effect, the broadening D of both spectral lines, emitting and absorbing, occurs (Figure 8.4); moreover, at room temperature, this broadening is of many orders of magnitude larger than the natural line width. As a result, only the tails of the spectral lines overlap; absorption will reach a miserable value from the expected effect.

Quite another picture is observed if both nuclei are confined in a crystal. In this case, the whole crystal needs to be considered as a closed system. The theory of this effect (at energies

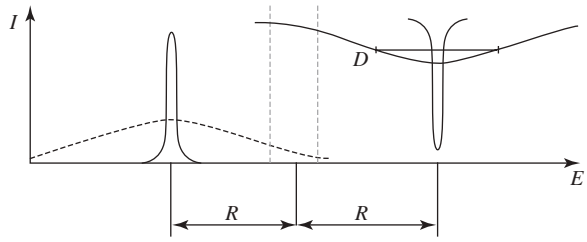

Figure 8.4 An infringement of the γ resonance.

of γ quanta smaller than the binding energy of atoms in the crystal) shows that, while emitting, two possibilities can arise. The first is the creation of an elastic wave in the crystal, i.e., phonon (refer to Section 9.3.1), which would carry away the excess of the energy of a γ quantum. This is inelastically scattered nonresonance quantum. The other possibility is an elastically scattered γ quantum, when the recoil energy is transmitted to the whole crystal.

Herewith, in the formula for the determination of R, instead of the nuclear mass, m_N, we should substitute the macroscopic crystal mass; then the recoil energy reduces practically to zero, and the γ-quantum energy becomes almost precisely equal to the energy difference $E_1 - E_0$. The Doppler broadening from the thermal motion also vanishes. As a result, the emitting and absorbing lines narrow down to the natural width and coincide with each other. The resonance requirement becomes satisfied.

The theory of this effect was worked out by R. Mössbauer (Nobel Prize, 1961) and the effect itself is referred to as the Mössbauer effect. It consists of *the recoilless emission and resonance absorption of γ quanta by nuclei.*

The ratio of the number of elastically emitted γ quanta to their total number is called the Mössbauer effect probability f and is proportional to:

$$f \sim \exp\left\{-\frac{\langle x^2\rangle \omega^2}{c^2}\right\}, \tag{8.3.9}$$

where $\langle x^2\rangle$ is a mean-square displacement of nuclei from their equilibrium position in a crystal as a result of their thermal motion (in the direction of quantum emission). The probability is proportional to the atomic mobility in a crystal.

How can γ-radiation resonance absorption be seen and measured? Assume that the emitter and absorber materials are quite similar and are in the same state. The maximum value of resonance absorption must be observed, when emitter and absorber are motionless ($V=0$) (eq. 8.3.2). When one begins to move, e.g., the emitter regarding the absorber, this resonance absorption is destroyed and the experiment reveals an absorption curve; a very small relative velocity is needed to "separate" the spectral lines (emitted and absorbed).

$$\frac{\Gamma}{\Delta E} \sim \frac{V}{c} \sim 10^{-12} \tag{8.3.10}$$

The relative velocity needed to destroy the resonance can be found from this equation. A striking result appears: despite the fact that light travels very fast, the speed needed to destroy the resonance is very small $V = c \times 10^{-12} = 10^{-4}$ m/sec! Therefore, the simplest way to observe resonance absorption is to measure it as a function of the relative speed, V. A schematic diagram of a ΓR experiment is presented in Figure 8.5a.

8.3.3 γ-Resonance (Mössbauer) spectroscopy in chemistry

As far as the volume of information that can be obtained on chemical and physical properties of chemical compounds, ΓRS occupies a leading position. Nuclear transitions correspond to energy difference 10^4 eV but the effect to be measured relates to 10^{-7}–10^{-8} eV; however, Mössbauer spectroscopy resolution is so high that it successfully solves such problems. In addition, this method can find nearly all the effects of nuclear interactions with an electronic shell; it carries extremely valuable information on molecular or crystal structure.

One of the main parameters of a resonance curve is its position on the velocity axis. In Figure 8.5a, a resonance curve is presented schematically when the emitter and absorber are one and the same motionless substance: the maximum of absorption falls on the zero value of relative velocity. Intensity of absorption (depth of curve minimum) is proportional to the probability of the resonance absorption, f. So, such measurements enable the measurement of a change in the atomic mobility in a sample under different treatments

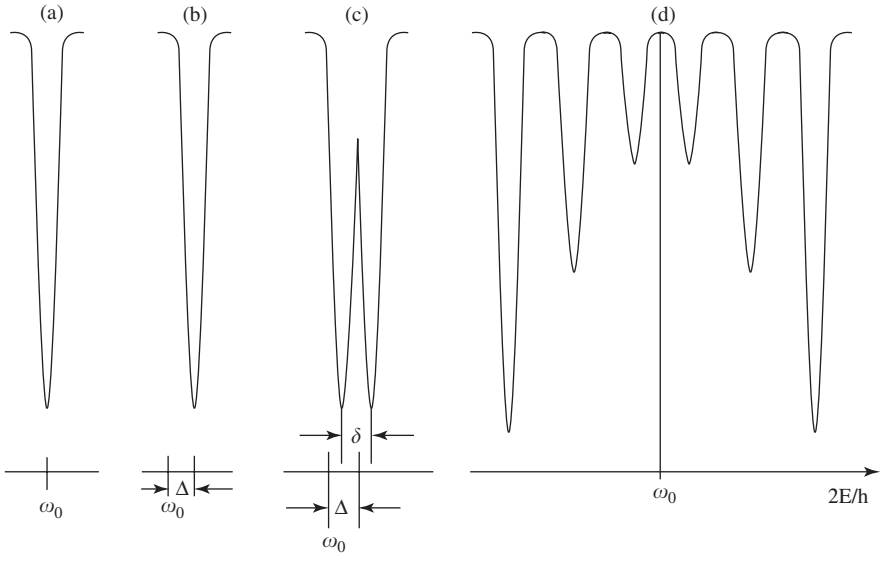

Figure 8.5 Exhibiting different effects in ΓR: (a) primary position of the absorption spectral line on the velocity axis by a stripped nucleus ω_0, (b) chemical shift $\Delta\omega$ (c) quadrupole splitting and (d) magnetic SF interaction development.

connected with such chemical problems as catalysts, chemisorption, polymerization and others.

If the source substance and absorber are different, the spectral absorption line is shifted along the velocity axis; that is caused by the additional energy E_{E_2} (8.2.9). The energy E_{E_2}, denominated in units of velocity, is called in ΓRS the *chemical shift* (Figure 8.5b). The sodium nitroprusside $Na_2[Fe(CN)(NO)_5]\cdot 2H_2O$ is mostly used as the standard (reference) substance in Mössbauer spectroscopy. Indication of the reference substance in scientific publications is obligatory.

If some atoms in a substance are in an asymmetric environment and their nuclei possess a quadrupole moment, quadrupole splitting can occur (Figure 8.5c). Knowing spin I, the splitting Δ allows the electric field gradient value of the nuclei that is dependent on the structure's peculiarities to be found.

If the substance under investigation is in a magnetically ordered state (ferro-, antiferro- or ferri-magnetic, refer to Section 5.3), a nuclear Zeeman effect takes place: energy levels split according to eq. (8.2.10). In Figure 8.5d, the case of a nucleus with $I=3/2$ in symmetrical surroundings in a magnetically ordered substance (e.g., antiferromagnetic, α-Fe_2O_3) is given. The number of lines allows the nuclear spin I to be found, whereas the distance between lines enables us to find the magnetic field induction (strength), created by the electronic shell, at the nucleus position $B(0,0,0)$ (or $H(0,0,0)$). The latter is a feature of electronic shell and differs for different atomic states.

Let us look at some examples. A particular interest for chemical investigations is the relative change of the chemical shift Δ in a number of various isostructural absorbers at a fixed (motionless) source. For example, one can judge the valence state of a Mössbauer atom in various compounds by measuring the chemical shifts. So, all bivalent tin compounds have positive chemical shifts relative to grey tin (the source of the radiation moves to the absorber), whereas all tetravalent compounds have a negative shift relative to grey tin (the source of the radiation goes from the absorber). The chemical shift value is proportional to the ionicity of a Mössbauer atom in the compound under investigation. In Figure 8.6, the spectra of a series of isostructural tin tetra-halogenides are presented with tetrahedrons SnI_4, $SnBr_4$ and $SnCl_4$, confirming this belief. However, from the same figure, it can be seen that there are no tetrahedrons with equivalent Sn–F bonds in the SnF_4 compound; a couple of resonance lines are present. Theoretical analysis of the spectrum obtained shows that there is a quadrupole electric super-fine interaction in this compound; this is explained by the reticular coordination polymer structure with nonequivalent Sn-F bonds (Figure. 8.6).

If a nucleus with energy E possesses a magnetic moment $\mathcal{M}$, which is in a magnetic field B, the energy of the nuclear state (8.2.10) will change by a magnitude ΔE. In ΓR experiments, the transitions between two different nuclear states are observed. As ΔE_M is proportional to the first order of m_I, the $(2I+1)$-fold degeneration is lifted in the magnetic field: to every m_I, there corresponds its own value ΔE_M. Distinction is measured in ΓRS effect at the transitions between the sublevels of two various nuclear states (Figure 8.2c). Thus, the number of lines of radiation/absorption spectra is defined by selection rules $\Delta m_I = 0, \pm 1$. For example, for nucleus ^{57}Fe and ^{119}Sn ($I_{ex}=3/2$, $I_{gr} = 1/2$) from eight formally possible transitions, only six are realized because of the selection rule.

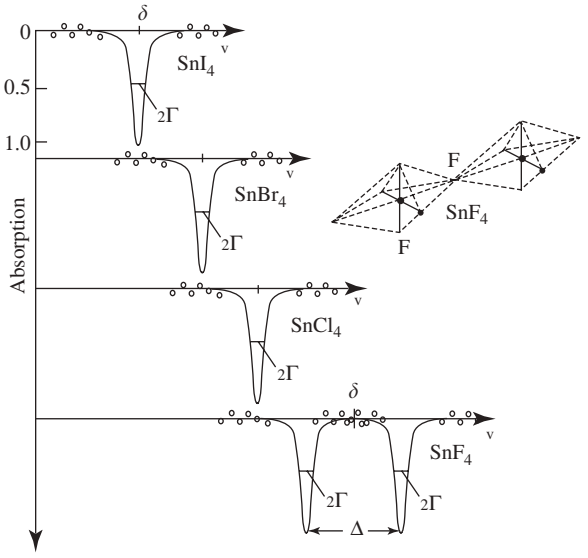

Figure 8.6 Results of a ΓRS investigation of tin tetrahalogenides. Quadrupole splitting is seen for SnF_4 (after E.F. Makarov *et al.*).

For chemical researchers studying magnetic fields acting on the nucleus of Mössbauer atoms, this is of essential interest as the magnetic field on the nucleus is caused by spin, radial and angular distributions of electronic density in an atom.

8.3.4 Superfine interactions of a magnetic nature

If an atom with a nucleus with a magnetic moment $\mathcal{M}$ appears in an inner field with magnetic induction B, the nuclear energy E (8.2.20) increases:

$$\Delta E_{\mathrm{M}} = -(\mathcal{M}B), \tag{8.3.11}$$

The transition between the two nuclear states is measured. As ΔE_{M} is proportional to the first degree of m_I, $(2I+1)$-fold degeneration is lifted, and a separate value of the energy level E_{M} corresponds to each quantum number m_I. This value is measured in ΓRS as the energy of the transitions between the sublevels of the two different nuclear states (Figure 8.2e). The number of spectral lines is the subject of limitation by selection rules $\Delta m_I = 0, \pm 1$ and depends on the number of energy lines in both ground and excited states.

It can be seen from eq. (8.3.31) that experimentally measured ΔE_{M} allows calculation of the magnetic field strength H (or induction B), which electrons of the same atom create on the nucleus. We will not discuss this event in more detail, but would like to underline that these fields appeared to be rather high (up to 10^5 A/m and even higher). In Figure 8.7, the

temperature dependence of ΓRS in ferromagnetic iron metal measurements is depicted: at elevated temperatures, all the SF spectral lines collapse into a single one; the crystal undergoes transformation to a paramagnetic state. The interline distance in spectra gives the magnetic field mentioned above.

8.4 NUCLEAR MAGNETIC RESONANCE (NMR)

8.4.1 Introduction

NMR consists of the resonance absorption of electromagnetic radiation by a system of nuclear magnetic moments of the substance under investigation. NMR was discovered in 1946 by E.M. Parcel and F. Bloch (Nobel Prize, 1952). At present, the method is widely used in chemistry because of its remarkable ability to solve many chemical problems.

There are several approaches to nuclear resonance descriptions. In this section, we will try to develop the energy approach, which is simpler for understanding. In Chapter 7.7 the behavior of a system of atomic magnetic moments in an external magnetic field was considered. Additional energy appeared; being applied to nuclei, this energy is $\Delta E = g_N \mu_N \Delta m_I B_0$, where g_N denotes the nuclear g-factor, μ_N is the nuclear magneton, m_I is

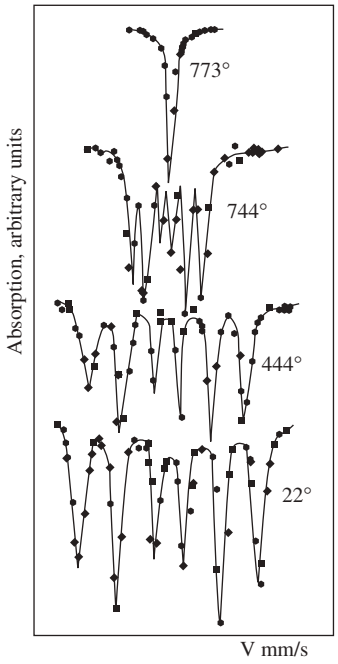

Figure 8.7 Magnetic ΓR experimental curves of iron heated to above T_C (see Section 5.3.1): all the SF lines collapse at $T > T_C$ (after E.F. Makarov *et al.*).

the nuclear quantum number that determines the projection of the magnetic moment vector onto the quantization axis and B_0 is the induction of the permanent external magnetic field applied to the substance.

The splitting of the ground state of the nuclear energy levels is the result of the nuclear Zeeman effect (Figure 8.2). This effect lifted the degeneracy of the ground state energy making it dependent on the quantum number, m_I. This means that the system that previously had one degenerated level, has $2I+1$ nondegenerate sublevels in the external magnetic field. For proton $I=1/2$, the number of sublevels is two with $m_I = \pm(1/2)$. Therefore, the ground state level will admit either positive or negative energy; in other words, it will be split, the splitting gap being

$$\Delta E = \mu_N g_N B_0 \tag{8.4.1}$$

(the quantum number m_I is absent in this equation because the transition difference corresponds to $\Delta m_I = \pm 1$). This is depicted by a grey double arrow in Figure 8.2e.

An alternating electric field with definite frequency is additionally applied onto the sample. This alternating field will be absorbed more intensively by the sample if the following resonance condition is achieved:

$$\hbar\omega_{res} = \Delta E = g_N \mu_B B_0 \tag{8.4.2}$$

There is a special coil to measure the absorption of an electromagnetic field.

There are many types of NMR apparatus available. Figures 8.8 depicted two main schemes: an old one (a) and greatly advanced one (b). Since a very stable magnetic field is needed, the superconducting magnetic coil (SMC) is constructed, merged into liquid helium. The special devices permit one to change samples without warming the main vessel. Moreover, they enable one to change the frequency range as well.

It can be seen from eq. (8.4.1) that the resonance condition can be met either by changing the frequency of the secondary alternating magnetic field at constant magnetic field B, or the induction variation B at constant frequency. Both possibilities can be realized in modern NMR apparatus. Sometimes it is easier to change the field (by means of sweep coils "*c*" in Figure 8.8a) and use the constant frequency. The majority of devices work according to these principles; actually, results do not depend on the choice of measurements.

The frequency ranges used are presented in Table 5.3.

So, the nuclear paramagnetic resonance NMR is the selective absorption of either the alternating electromagnetic energy in the presence of a permanent magnetic field by a substance containing atoms whose nuclei have nonzero spins, or vice versa, the absorption of magnetic induction B at constant frequency of the alternating field.

8.4.2 Use of nuclear magnetic resonance in chemistry

In order to realize the resonance absorption of an alternating magnetic field, one should have a sample with nuclei that possess nonzero magnetic moments, i.e., nonzero spin quantum number. The nuclei ^{1}H (protons), ^{11}B, ^{13}C, ^{19}F and some others have such nonzero

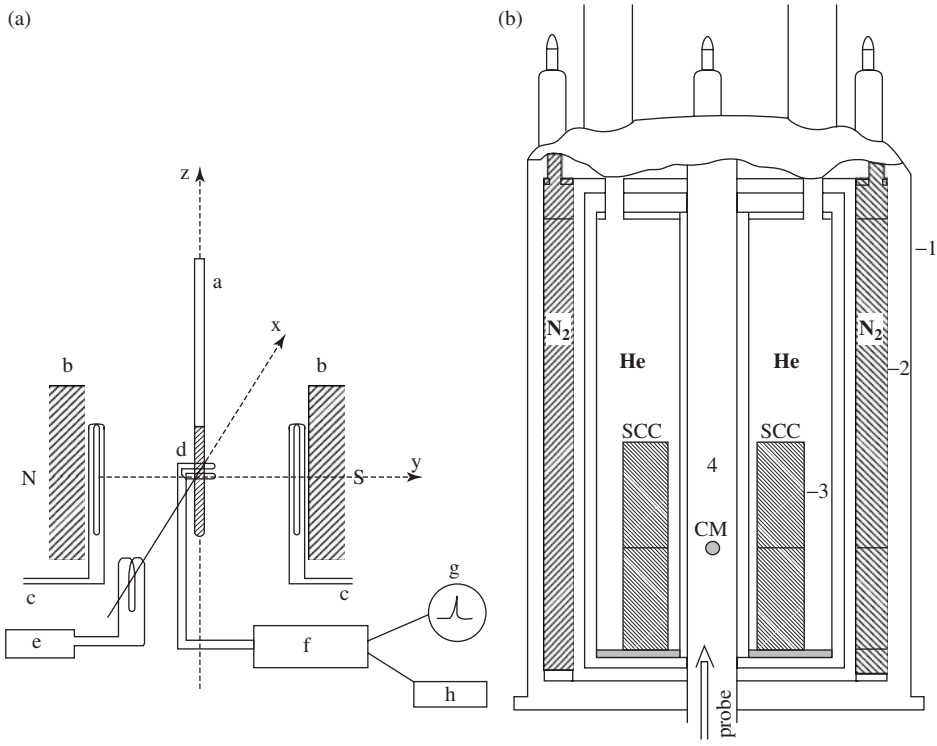

Figures 8.8 Schemes of NMR spectrometers. (a) An original old spectrometer scheme of the continuous wave (a: sample tube; b: magnet; c: sweep coil; d: receiver coil; e: transmitter; f: amplifier; g: register unit; h: recorder), the electromagnet poles are also seen. (b) Section of a more advanced NMR spectrometer, the nitrogen and helium vessels with the superconducting magnetic coil are depicted. A sample is introduced from above; however, the device (probe), inserted from below, realizes the connection of sample measurement coils with the register system. CM: position of the sample investigated.

spins. It can be seen that many atoms dealt with in modern chemistry are present in this list. Proton magnetic resonance (PMR) is most popular in chemistry, but resonance on ^{19}F and ^{13}C is also often used. However, the information quality is so great that using the spectra of these atoms, one can find the behavior of other atoms of the mother molecule.

Consider the behavior of hydrogen nuclei (protons) in atoms in a certain molecule in the external magnetic field, B_0. The proton spin quantum number is 1/2, therefore, its lower energy level is split (Figure 8.2e).

The purpose of the constant magnetic field is to split the single level in two due to the nuclear Zeeman effect. The alternative electromagnetic field $B(\omega)$ facilitates transitions between sublevels. The third coil is to measure absorption. The principle difference between NMR and ΓRS is as follows: on account of its enormous resolution, γ resonance allows one to define the superfine structure investigating the transition between different nuclei states (levels) with different I, whereas NMR allows one to measure the transition

between sublevels of one and the same ground level. So, in spite of the difference between the methods, the results obtained often have the same nature.

Consider the PMR ability using the example of the ethyl alcohol molecule CH_3–CH_2–OH. It contains six protons in three different atomic groups. However, only hydrogen protons give a contribution to the spectrum in the given frequency range.

The PMR spectrum of ethyl alcohol obtained by a spectrometer with a very low resolution would contain only one spectral line to which all the protons contribute simultaneously. The information that can be obtained from such a spectrum is restricted by the statement that in fact there are hydrogen atoms in the sample. Substitution of hydrogen by, say, fluorine atoms would remove the signal completely.

By improving the spectrometer resolution, the amount of information can be significantly increased. Consequently, it can be found that protons of different atomic groups absorb an electromagnetic wave under a different external magnetic field (Figure 8.9a). The amount of information in such a spectrum increases: the presence of three maxima shows that there are three types of hydrogen atoms in a compound, the resonance for different functional groups CH_3, CH_2 and OH takes place at the three different experimental conditions. This is because of the fact that, as well as the outer magnetic field, an additional magnetic field acts on each proton. The origin of these additional fields is the diamagnetic response of the given atom to the external field. Every particular atom has its

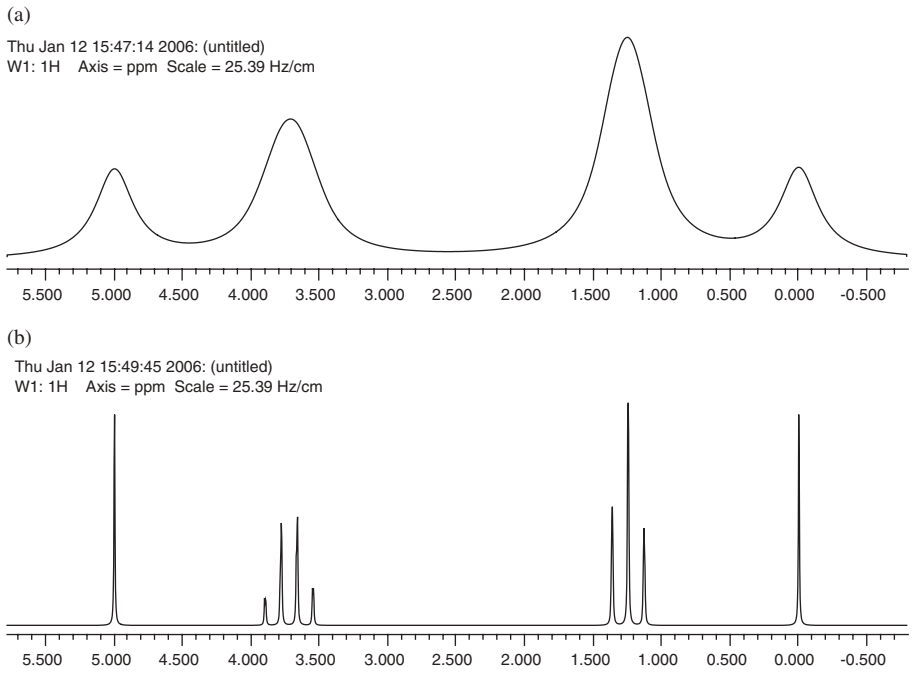

Figure 8.9 The NMR spectra of ethyl alcohol obtained at intermediate (a) and higher (b) resolution. Zero position signal corresponds to TMS.

own electron cloud subject to some individual changes under the influence of the chemical bonding. This diamagnetic field is local, i.e., different for different atomic groups.

How small the differences in the electron shell of hydrogen atoms in different positions, this difference is exhibited in the diamagnetic screening of the given nucleus. This signifies that not only will the external magnetic field with the induction B_0 act on the given proton, but an additional local field as well, specific only to this particular atom.

It was shown in Section 5.2 that the diamagnetic field is proportional to the external magnetic field and is in the opposite direction to it. Thereby,

$$\begin{aligned} B_A &= B_0 - \sigma_A B_0 = B_0(1-\sigma_A), \\ B_B &= B_0 - \sigma_B B_0 = B_0(1-\sigma_B), \\ B_C &= B_0 - \sigma_C B_0 = B_0(1-\sigma_C), \end{aligned} \tag{8.4.3}$$

where A, B and C show the structure-nonequivalent atoms of hydrogen in the molecule. σ-Values are screening constants; they depend upon the electron structure, which, in turn, depends on more distant effects of the influence of the neighboring atoms and atomic groups. Dimensionless values σ correspond to atomic diamagnetic susceptibility; they are of the order 10^{-6} (this value's order dictated the high requirement of magnetic field stability). On the background of unity, this is a very small value; nevertheless, it is reliably measured in an experiment. This is because of the fact that being in the outer magnetic field B_0, protons of the hydrogen atoms "fill" not that field but fields B_A, B_B, B_C, etc. Consequently, resonance occurs under some field other than B_0 (at a fixed frequency). Thereby, the NMR spectrum *consists of as many spectral lines as the structure-nonequivalent hydrogen atoms present in the molecule*: for each of them, resonance will be observed under the different induction of the magnetic field.

Such displacement of the position of the NMR signal along the magnetic induction axis depending on the atomic electron shell properties is referred to as the *chemical shift*.

NMR spectrum of the same ethyl alcohol molecules is given in Figure 8.9b measured by a high-resolution NMR spectrometer. It can be seen that the proton resonance of the different functional groups CH_3, CH_2 and OH takes place at different values of the magnetic field (on account of the difference in σ). There follows, in particular, an important conclusion that the number of NMR signals on the spectrum is equal to the number of structure-nonequivalent protons in the molecule. (For instance, in benzene there will be one signal, in mono-substituted benzene there will be three, in ortho-di-fluorine-benzene—one, in para-di-fluorine-benzine—one, in meta-di-fluorine-benzine—two, etc).

It would be useful to impart a quantitative meaning to the notion of the "chemical shift" in NMR. For this purpose, for instance, it was possible to obtain an NMR signal for a "stripped" proton and measure the shift from its signal. However, it is too complicated to obtain a signal from a "necked" proton, particularly for every sample. It was agreed, therefore, to choose a standard "reference" substance. At present, tetramethilsilan $Si(CH_3)_4$ (TMS) has been chosen as the most widespread standard substance. This substance has many advantages. Firstly, there is a relatively large amount of hydrogen in this compound.

Secondly, all protons of methyl groups are structure-equivalent, so TMS exhibits itself by only one NMR signal. Thirdly, in solutions the CH_3 groups revolve around the Si–C bonds and, therefore, the magnetic fields are averaged and the TMS signal is very narrow. Fourthly, the screening constant of the methyl group is minimal with respect to the majority of other hydrogen-containing substances. Consequently, the TMS reference line lies nearly always on the right side on all other signals on the axis of the magnetic field induction. From this line, the chemical shift is always positive (measured to the left side).

To compare chemical shifts obtained on different instruments with different working frequencies, it was accepted to express the chemical shift quantitatively in relative units (in millionth units, or in m.u.) (not dependent neither on B_0 nor ω_0):

$$\delta_i = \frac{B_{0i} - B_0(\text{TMS})}{B_0(\text{TMS})} \times 10^6, \tag{8.4.4}$$

where B_{0i} and B_0 (TMS) are the induction of external magnetic fields corresponding to the resonance absorption at the principle frequency of the group of equivalent nuclei (i) of molecules under investigation and in TMS, correspondingly. Thereby, δ_i is defined by the relative displacement of the NMR signal of a given molecule on the spectrum to the left from the TMS lines. The evaluation shows that, for the hydrogen atom, removing one s-electron brings about a chemical shift of 20×10^{-6} or in 20 m.u. Therefore, δ_i for protons in the majority of different atomic groups have values from 0 to 10 m.u.

There exist other, less often used, scales of chemical shifts. The generalization of NMR spectra allows experimental results on chemical shifts to be exhibited in the form depicted in Figure 8.10. Since the protons in similar atomic groups have somewhat different δ, the chemical shift values are plotted on the abscissa axis in the form of segments (not points) of δ_i (in m.u.); the corresponding functional atomic groups are plotted on different levels on the ordinate axis. The black strips correspond to those cases, which are met with more often.

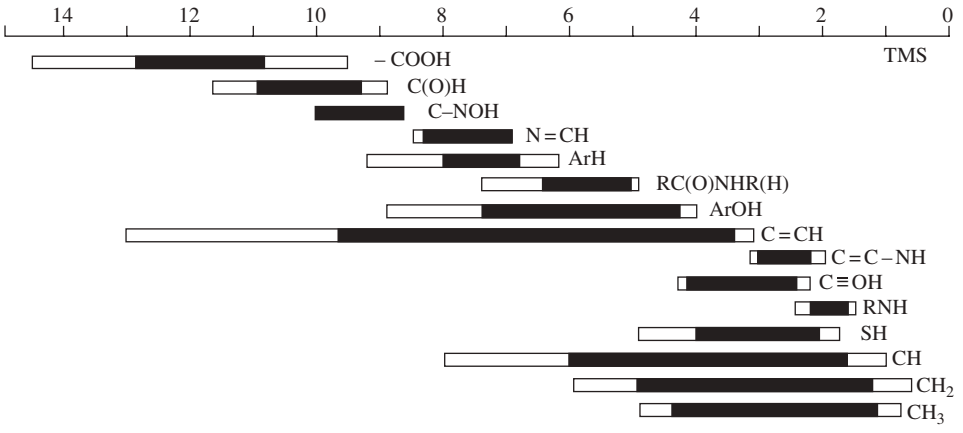

Figure 8.10 Generalization of the proton chemical shift in different atomic groups.

Having obtained a PMR spectrum, the information can be used to gain a representation of whatever substance is being dealt with. Similar tables are accumulated for other nuclei as well.

The picture described, however, is equitable only in some respects. There actually exist other finer effects influencing the spectrum. The mutual interaction of the proton magnetic moments of different functional groups can be mentioned in the first order. This interaction turns out to be stronger than was assumed, keeping in mind the interaction between two nuclear magnetic moments (magnetic dipole–dipole interaction). This is because magnetic moments of protons superpose magnetization onto electrons, participating in the chemical bonding in the molecule (particularly, electrons participating in chemical coupling), which, in turn, creates a magnetic field on the neighboring proton. This additional chemical bond magnetization noticeably enlarges the hydrogen proton chemical shift, as well as enlarging the interaction between proton containing groups, and does its more long-range acting. Such a type of interaction is called a spin–spin interaction.

Spin–spin interaction is exhibited in the high-resolution spectrum. The spectrum gets more complicated whereas the information on the molecular structure increases.

Let us consider this phenomenon using the example of the same ethyl alcohol, measured on the high-resolution spectrometer (Figure 8.9b). As has already been noted, three types of hydrogen groups manifest themselves in three line series, belonging to protons of different functional groups. The one right utmost line is a mark of resonance in TMS ($\delta=0$). The group of lines at $\delta\approx1.2$ m.u. corresponds to protons of the CH_3, the group of lines at $\delta\approx3.5$ m.u. corresponds to the group CH_2, and at $\delta\approx4.5$ m.u. to the OH group.

Let us look at the spin–spin interaction between protons of three functional groups in the molecule of ethyl alcohol. The proton can occupy two positions in the external field with projections defined by quantum numbers $m_I=\pm(1/2)$. Denote the state with $m_I=+1/2$ by the letter α and with $m_I=-1/2$ by the letter β.

Analyze first the action of protons of group CH_2 on the nearest groups, CH_3 and OH. Two protons of CH_2-groups can accept three total quantum numbers, S:

$$\begin{aligned} &\alpha\alpha\text{-spin} = +1 && S = 1,\\ &\alpha\beta\text{-and}\,\beta\alpha\text{-spin} = 0 && S = 0,\\ &\beta\beta\text{-spin} = -1 && S = -1, \end{aligned}$$

the total number of states with $S=0$ being twice as large as the other S values. Correspondingly, the neighboring lines of the CH_3 and OH groups split into three with relative intensity 1:2:1 (Figure 8.9b).

Evaluate now the action of CH_3 on the protons of their neighbors. The number of states of the group of three protons can have four values of the total S:

$$\begin{aligned} &\alpha\alpha\alpha\text{-spin} = \tfrac{3}{2} && S = \tfrac{3}{2},\\ &\alpha\alpha\beta,\ \alpha\beta\alpha,\ \beta\alpha\alpha\text{-spin} = \tfrac{1}{2} && S = \tfrac{1}{2},\\ &\alpha\beta\beta,\ \beta\alpha\beta,\ \beta\beta\alpha\text{-spin} = -\tfrac{1}{2} && S = -\tfrac{1}{2},\\ &\beta\beta\beta\text{-spin} = -\tfrac{3}{2} && S = -\tfrac{3}{2}, \end{aligned}$$

with the relative number of states 1:3:3:1, accordingly. The SF dipole–dipole splitting is depicted in Figure 8.11 (without following the scale on). Consequently, the influence of group CH_3 on group CH_2 will be exhibited in the splitting of the signal. The action of the hydroxyl group in a favorite case obeys the general rule herewith each of the four lines must else be split into two. So, the high-resolution signal of the group CH_2 in the ethyl alcohol is usually split into eight components. The general rule for nuclei with $I=1/2$ corresponds to this example: the number of spin–spin splitting caused by spin–spin interaction, is $n+1$, where n is the number of protons in the adjacent atomic group whose influence is considered (in the general case with $I>½$, this number is $2nI+1$). This phenomenon can be described quantitatively by the spin–spin interaction constant J, proportional to the distance between the lines of the spin–spin splitting in the spectrum. Unlike the chemical shift, J does not depend on inductions of magnetic field B_0 and so it is expressed right in Hz. For many atomic groups, J is well known and is reported in reference books.

If, in the molecule in the main atomic group alongside the protons, there are other atoms with magnetic nuclei they can participate in spin–spin interaction not exhibiting their own magnetic moments. In this case, the splitting character is more complicated, though the amount of information on the substance increases as well.

The above-considered example of the PMR spectrum of ethyl alcohol is equitable only for very pure material. If a small admixture of water is present in the sample, the OH group will not be exhibited in the spectrum. This is because the proton of the hydroxyl group

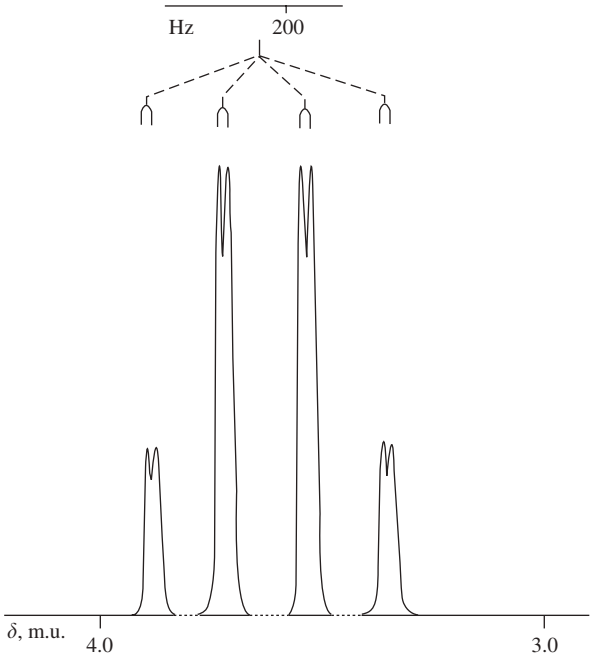

Figure 8.11 The scheme of a SF nuclear dipole–dipole splitting (scale not followed).

sometimes participates in the rapid exchange between the alcohol and water molecules. The time of exchange influences the width of the PMR signal. Depending on the rate of this exchange, a signal can be significantly broadened or disappear completely. This also illustrates the possibilities for PMR in chemical applications.

In the last decade, some methods have been offered that are more complex and significantly more informative. In particular, a number of methods have greatly increased the ability of NMR (R.R. Ernst, Nobel Prize, 1991). Ernst found that the ability of NMR, previously limited by the small number of nuclei, could be greatly extended by substituting a slow variation of the magnetic field by strong short pulses, decomposed by means of Fourier transformations in a certain number of harmonics. Thereby, for one pulse, a field runs the whole spectrum of frequencies. The inverse Fourier summations permit a normal NMR spectrum to be obtained. The method allows greatly enlarged sensitivity of the NMR spectroscopy and involves a greater number of nuclei. The method allows influence upon the processes of spin–spin interaction, enlarging or reducing their intensity. A method of two-dimensional scan has also been worked out with the participation of R. Ernst. This approach permits one to influence the spin–spin interactions, enlarging and/or suppressing them. This enables one to untangle complex spectra of polymeric and biological objects.

A mechanism of spin–lattice and spin–spin relaxations was also worked out at the same time. The point is that the relative levels occupancy N''/N', between which a transition occurs, is defined by the Boltzmann factor. The probability of transition between two levels is greater the larger the distance between them and, consequently, the more N''/N' differs from 1. In γ-gamma resonance, the energy difference is of the order of 10^4 eV, so the upper level is always nearly free and resonance absorption of quantum is nearly always possible. In NMR resonance, the difference $E''-E'$ is extraordinarily small and factor N''/N' is close to 1. Under such conditions, the occupancy of both levels is the same and the probability of transition should be very small; and, basically, paramagnetic resonance must not be observed. However, it turns out that another mechanism of removing the excitation from the upper level exists.

Two such processes are the excitation of either thermal crystal lattice oscillations (spin–lattice relaxation) and/or excitement of oscillation in the nuclear magnetic system (spin–spin relaxation). Both processes are characterized by constants $T1$ and $T2$: $T1$ is the spin–lattice relaxation time and $T2$ is the spin–spin relaxation time. Values of $T1$ and $T2$ render an essential influence upon the form of resonance curves. On the other hand, the relaxation processes depend on the mobility of one atomic group or another in the substance. So, experimental measurement of the relaxation processes serves as a method of measurement of the dynamics of chemical conversions depending on time, temperature, chemical conversion particularity and other factors.

New, rather complex instruments—tomographs—have been constructed on the basis of NMR. They can be successfully applied in the medical diagnosis of normal and pathological human tissues. The general principle of tomography consists of the fact that the amplitude of the NMR response is proportional to the proton concentration in the sample investigated. In the human body, hydrogen is present in water and in adipose tissue; in the latter, its percentage being higher than in water. So, in picture imaging the distribution of hydrogen, one can see a distinct contrast between adipose and other tissue. To increase contrast, another characteristic of the NMR signal can be used: the strong dependence of the relaxation times on the chemical composition of the medium.

Being practically harmless, NMR is used for the diagnosis of pathology in the human body, particularly for the hard-to-reach parts of the body such as the heart, liver and brain.

8.5 ABILITIES OF NUCLEAR QUADRUPOLE RESONANCE

NQR is a method based on the resonance absorption of electromagnetic energy in a substance owing to quantum transitions between nuclear energy levels, created by a nuclear quadrupole moment interaction with the gradient of the intracrystal electric field (Section 8.2.4, Figure 8.2c). NQR has been developed on account of the interaction of the electrical field gradient of the shell electrons with the gradient of electrical field appearing because of nonspherical electron density in atoms (refer to Appendix 3). Quadrupole interaction brings about a change in the energy states, corresponding to nuclear spin different spatial orientation regarding the crystallographic axes (formula (8.2.10)). An alternating electromagnetic field causes a magnetic dipole transition between sublevels of the main level, which is found as resonance absorption of electromagnetic energy. Since the energy of quadrupole interaction changes are in rather broad limits depending on the nuclear characteristics and on crystal structures, so the NQR frequencies lie in a range from hundreds kHz to thousands MHz.

At present, NQR is not used as widely in science and technology as NMR. Nevertheless, many questions can be solved more quickly and easily with NQR than by NMR, not least because this method does not require an external magnetic field and availability of single crystals. NQR measurements are characterized by a high spectral resolution, selectivity and rate. In particular, of current importance is the remote control of air on the presence of different nitrogen compounds by means of NQR.

Nuclear charge quadrupole moment eQ interacts with the gradient of electrical field, e^2Qq, defined by an asymmetry parameter, η; it contains information on the molecular structure. These parameters can be determined from experiment.

The NQR method can also be used in solids and, predominantly, crystals.

There are four areas of successful investigation: electron density studies in molecules, in particular, changes in the orbital occupancy at complexation and substitutions, study of molecular dynamics, in particular, reorientation, rotation of atomic groups, hindered rotation, phase transformation study, revealing and studying defects and mixed crystals investigation.

The NQR method is used in nuclear physics for the determination of nuclear quadrupole moments. In crystal chemistry, the method gives information on symmetry and structure, macromolecules ordering degree, their motion and nature of chemical bonding. The method permits the definition of a number of structure-nonequivalent atoms even with nonzero quadrupole moments. While with the NMR method, the structure of a molecule manifests itself only as broadening and splitting of lines; with NQR measurements, the crystal structure is defined by resonance frequencies themselves. Since in NQR, there is a distinctively strong dependence of the spectral line width from defect concentration in crystals; the line-width measurement allows the study of internal stresses in the crystal, the presence of admixtures and ordering processes. The parameter of asymmetry strongly depends on structures; so, in particular, in an ion $NC_2H_2^+$, when substituting two hydrogen atoms on carbon, it is changed from 0 to 1, which is easy to observe in an experiment.

EXAMPLE E8.1

Calculate the relative emitter/absorber velocity V requires to compensate recoil energy and observe resonance on a free ^{197}Au isotope (wavelength is $\lambda = 0.016$ nm).

Solution. In order to destroy the resonance, one can move the resonance line on its width Γ (eq. (8.3.10)) taking into account the fact that the recoil process relates both to emitter and to absorber. Therefore, to compensate for this effect, it is necessary to move one of them with velocity V, which can be determined according the equation:

$$\hbar\omega \frac{V}{c} = 2R.$$

Therefore,

$$V = \frac{2Rc}{\hbar\omega} = 2\frac{(\hbar\omega)^2 c}{2m_N c^2 \hbar\omega} = 2\frac{2\pi\hbar}{2m_N\lambda} = \frac{h}{m_N\lambda}.$$

Substituting all known values into this equation, we arrive at $V = 126$ m/sec. This value is not small, however, in comparison with quantum speed $(V/c) \sim (0.1/10^8) = 10^{-9}$, which seems negligible.

EXAMPLE E8.2

The spin quantum number of a nucleus of ^{14}N is $I = 1$. Therefore, the nucleus has three energy levels with frequencies ν_0, ν_+ and ν_+ (for $m_I = +1, 0, -1$, correspondingly). Two frequencies of ^{14}N in sodium nitrate ($NaNO_2$) are $\nu_+ = 4.640$ MHz and $\nu_- = 3.600$ MHz. Calculate (1) NQR frequency ν_0, (2) asymmetry parameter η and (3) quadrupole coupling constant $e^2q_{zz}Q/h$.

Solution. (1) A simple average ν_0 can be easily calculated $\nu_0 = \nu_+ - \nu_- = 1.040$ MHz. (2) The quadrupole moment is $\nu_+ = 3/4(e^2q_{zz}Q/h)(1+\eta/3)$, $\nu_- = 3/4\ (e^2q_{zz}Q/h)\ (1-\eta/3)$: the solution of these two equations give: $\eta = 3(\nu_+ - \nu_-)(\nu_+ + \nu_-) = 0.38$. (3) The quadrupole moment of ^{14}N is: $\{(e^2q_{zz}Q/h) = 2(\nu_+ - \nu_-)/\eta] = 5.474$ MHz

8.6 ELECTRON PARAMAGNETIC RESONANCE (EPR)

The effect of resonant absorption of electromagnetic waves by electron paramagnetic centers in a substance in a permanent magnetic field is referred to as electronic paramagnetic resonance (EPR).

In the EPR method, the resonance condition for electrons looks like that for nuclei (refer to eq. (8.3.1):

$$E_1 - E_0 = \hbar\omega_{res} = g_E\mu_B B, \tag{8.6.1}$$

though instead of nuclear, electron characteristics are included. A comparison of resonance in nuclear and electronic subsystems (see Section 8.3.1) shows that the frequency of the EPR-resonance used is higher than that in NMR, i.e., it is approximately 10^9 Hz, which corresponds to the wavelength 10^{-1} m (several centimeters) lying in the microwave range (see Table 5.3). In EPR, an external permanent magnetic field influences electron spin energy level split; however, a high-frequency field throws the spins from one state to another. In other words, the external permanent magnetic field removes degeneration from electron energy states on quantum number m_S.

The basic EPR circuit is similar to that for NMR though the technique of EPR measurements differs significantly from that of NMR.

Intraatomic superfine interaction is described differently depending on the aggregative state of the substance investigated. In particular, it has the same nature in liquids as that described in Section 8.3 and is referred to as *contact interaction*; it is described by the term:

$$a \cong \frac{8\pi}{3}\frac{\mathcal{M}_I}{I}\left|\psi(0,0,0)\right|^2 \tag{8.6.2}$$

It can be seen that contact interaction is caused mostly by s-electrons, because only for s-electrons is the wave function on the nucleus distinct from zero. However, contact interaction of the same character can be observed in some cases in the absence of a noncoupled s-electron; it can arise to the account of π-electron of aromatic hydrocarbons belonging, for example, to anion-radicals: contact interaction of a nucleus with s-electrons is rather sensitive even to small electron excitation at hybridization.

The interaction of noncoupled electron spins with the nucleus can cause SF EPR line splitting EPR signal. The character of the splitting, or SF splitting of the EPR signal, is defined by a nucleus spin interaction with the number of specific atomic configuration in the nearest neighborhood. For a proton, the rule $n+1$ (where n is the number of nonequivalent atoms) is valid in this case as well, since $I=(1/2)$, like electron spin.

The simplest case is atomic hydrogen where SF splitting is defined by electron interaction with a nucleus (proton) belonging to the same atom. Notice that the reorientation time of a nucleus in an alternating magnetic field is much longer than the corresponding electron time. This means that the nuclear spin assigns the quantization axis and electron spin reorients alone (transition from $m_S=+1/2$ to $m_S=-1/2$). Quantum numbers for an electron spin and proton are identical and equal to 1/2. This means that the number of possible states is equal to two (spin of an electron and nucleus are parallel, the coupled spin is 1; or antiparallel, the coupled spin is zero). Therefore, the EPR spectrum of an atomic hydrogen consists of two SF signals (Figure 8.12a) split on 502 Oe (remember that the size of splitting does not depend either on the external field or on frequency). A deuteron's spin quantum number is equal to 1. Therefore, there are three possible mutual orientations of the deuteron and electron spins resulting in 1, 0 and –1. Hence, the EPR signal of atomic deuterium consists of a three-line SF structure divided by a field 78 Oe (Figure 8.12b). The splitting is proportional to a; this allows one to determine the magnitude $|\psi(0,0,0)|^2$ for hydrogen (deuterium) atoms. Notice that the rule $n+1$ for a deuteron is no longer valid, since $I>1/2$.

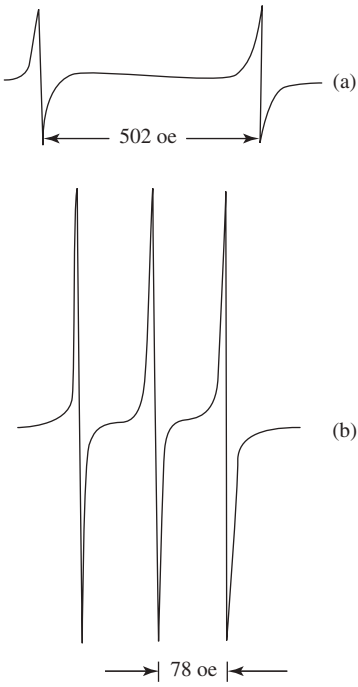

Figure 8.12 EPR spectra of atomic H (a) and D (b).

The EPR spectrum of each atom, ion or radical, has a specific shape (due to SF electron–nuclear interaction) well known to experts and given in the specialist reference literature. The most successful fields of application of the EPR method are: atoms and radicals (stable and/or unstable) with odd number of electrons, short-lived particles as elements of intermediate stages of the chemical reactions, ions of transition elements with partly built-up electron shells, crystal defects, etc. Integral signal intensity is proportional to paramagnetic center number; hence, the EPR spectrum contains important characteristics of a substance, such as the concentration of free radicals, number of defects of a crystal lattice, etc. The position of a signal allows one to determine the *g*-factor of a paramagnetic atom. Therefore, one can find the state of the paramagnetic center (refer to Section 7.6.2). Notice that, in view of relativistic effects, the spin *g*-factor is not precisely to 2, but is 2.0023.

PROBLEMS/TASKS

8.1 A free ^{40}K nucleus emits a γ-photon with the energy $\varepsilon_\gamma = 30$ keV. Find the relative displacement $\Delta\lambda/\lambda$ of the spectral line due to nucleus recoil.

8.2 A ^{67}Zn nucleus with the excitement energy $\Delta E = 93$ keV emits a γ-photon transferring from the excited to the ground state. Determine the relative change of $(\Delta\varepsilon_\gamma/\varepsilon_\gamma)$ of the γ-quantum energy because of the recoil of the initial nucleus.

8.3 Calculate an atom's recoil energy R after emission photon in (1) visible range energies (λ=500 nm), (2) in X-ray range (λ=0.5 nm) and (3) in γ range ($\lambda=5\times10^{-3}$ nm). Consider one and the same nucleus of mass m=100 a.u.m.

8.4. The atomic bonding energy E_b in a crystal is E_b = 20 eV; atom mass is 20 a.m.u. Find the minimum quantum's energy, which kicked the atom out of the crystal.

8.5. Simulate the ΓR spectrum of ilmenite ($FeTiO_3$) if iron's chemical shift δE_I relative to stainless steel is 1.3 mm/sec and the quadrupole splitting ΔE_Q=0.5 mm/sec. The Fe excitation energy is 14.4 keV. Express δE_I and ΔE_Q in eV units.

ANSWERS

8.1. $\Delta\lambda=1.7\times10^{-17}$; $(\Delta\lambda/\lambda)=(\varepsilon_\gamma/2m_Nc^2)=4\times10^{-7}\,m$.

8.2. $\Delta\varepsilon_\gamma/\varepsilon_\gamma=(\varepsilon_\gamma/2m_Nc^2)=7.45\times10^{-7}$.

8.3. $R=\dfrac{2}{m_A}\left(\dfrac{\pi\hbar}{\lambda}\right)$; (1) 33 peV; (2) 33 meV; and (3) 0.33 eV.

8.4. $\varepsilon_\gamma=c\sqrt{2m_NE_b}=8.6\times10^{-5}$ eV .

8.5. δE_I = 6.24 × 10^{-8} eV, ΔE_Q = 2.4 × 10^{-8} eV.

This page intentionally left blank